Biomass and Bioenergy 91 (2016) 48–55

Contents lists available at ScienceDirect

Biomass and Bioenergy

journal homepage: http://www.elsevier.com/locate/biombioe

Research paper

Fractional pretreatment of raw and calcium oxalate-extracted agave bagasse using ionic liquid and alkaline hydrogen peroxide

José A. Perez-Pimienta [a], Héctor M. Poggi-Varaldo [b], Teresa Ponce-Noyola [a, *], Ana C. Ramos-Valdivia [a], José A. Chavez-Carvayar [c], Vitalie Stavila [d], Blake A. Simmons [e, f]

[a] Department of Biotechnology and Bioengineering, Cinvestav-IPN, Ciudad de México, Mexico
[b] Environmental Biotechnology and Renewable Energies R&D Group, Dept. Biotechnology and Bioengineering, Cinvestav-IPN, Ciudad de México, Mexico
[c] Materials Research Institute, UNAM, Ciudad de México, Mexico
[d] Sandia National Laboratories, Energy Nanomaterials Department, Livermore, CA, United States
[e] Joint BioEnergy Institute, Physical Biosciences Division, Lawrence Berkeley National Laboratory, Emeryville, CA, United States
[f] Sandia National Laboratories, Biomass Science and Conversion Technology Department, Livermore, CA, United States

ARTICLE INFO

Article history:
Received 4 August 2015
Received in revised form
29 April 2016
Accepted 1 May 2016
Available online 10 May 2016

Keywords:
Agave bagasse
Calcium oxalate
Biomass pretreatment
Ionic liquid
Hydrogen peroxide

ABSTRACT

Occurrence of calcium oxalate (CaC_2O_4 – CaOX) crystals has been observed in more than 215 plant families. However, very little is known about the effects of calcium oxalate on biomass pretreatment and saccharification. Agave bagasse (*AGB*) was used as a model material due to its natural high levels of CaOX. To understand the physicochemical changes in function of biomass pretreatment, both raw *AGB* and CaOX-extracted agave bagasse (*EAB*) were subjected to ionic liquid (*IL*) with 1-Butyl-3-methylimidazolium chloride [C_4C_1Im][Cl] and alkaline hydrogen peroxide (*AHP*) pretreatments. Physicochemical changes were monitored by X-ray diffraction (XRD), Fourier transform infrared spectroscopy (FTIR), and wet chemistry methods. Results show that free CaOX crystals affected negatively (by ca 39%) the saccharification of *AHP*-pretreated *EAB* compared to *AGB*. On the other hand, *IL* pretreatment achieved higher sugar yield (7.8 g dm^{-3}) and lower crystallinity (14%) with *EAB* than for *AHP* (5.4 g dm^{-3} and 29%, respectively).

1. Introduction

Lignocellulosic biomass is currently considered the most promising long-term feedstock for biofuels production, however, it is highly recalcitrant to breakdown and offers limited accessibility to enzymatic degradation of cell wall sugars and subsequent fermentation [1]. Pretreatment by deconstructing the biomass is crucial, but is still a quite costly process that liberates fermentable sugars from biomass. A suitable pretreatment process involves: (1) disrupting hydrogen bonds in crystalline cellulose, (2) breaking down cross-linked matrix of hemicelluloses and lignin, (3) raising the porosity surface area of cellulose, and finally, (4) avoiding the formation of byproducts that are inhibitory to subsequent processes [2,3].

Several pretreatment technologies are employed to overcome lignocellulose recalcitrance and can offer high selectivity in deconstructing biomass to desired end products by partially breakdown the plant cell wall to improve enzymatic accessibility. A number of processes are currently available to pretreat lignocellulosic biomass; some key examples use liquid catalysts such as acids (H_2SO_4 or HCl), ammonia, bases (such as NaOH or H_2O_2), ionic liquids (such as 1-Butyl-3-methylimidazolium chloride [C_4C_1Im][Cl] or 1-ethyl-3-methylimidazolium acetate [C_2C_1Im][OAc]) or simply water. It has been a considerable challenge to clarify the physicochemical effects of the diverse types of pretreatments upon subsequent hydrolysis and fermentation [4].

Lignocellulosic feedstock such as Agave plants growing in arid and semi-arid lands could be a sustainable response to the growing demand for renewable fuels that do not conflict with food production. Such plants use Crassulacean Acid Metabolism (CAM) and therefore have low water requirements and are productive in semiarid regions. Therefore as carbon is assimilated overnight thereby decreasing the diffusive gradient of water out of the leaves and improve water use efficiency [5,6]. Due this efficient use of resources, CAM plants have recently been introduced as potential bioenergy crops [7]. The high soluble carbohydrate reserves that

* Corresponding author.
E-mail address: tponce@cinvestav.mx (T. Ponce-Noyola).

http://dx.doi.org/10.1016/j.biombioe.2016.05.001
0961-9534/

CAM plants contain, requires less energy for conversion to fuels hence resulting in a better quality material. With regard to future climate change, species of agave may have an advantage over other bioenergy crops (such as sugarcane or corn stover) because CAM physiology adapts to extreme temperatures and drought. Interestingly, the areas in the world that have been identified as most suitable for Agave plantations as feedstock (Mexico, Australia, and South Africa) are also areas where the variation in the temperature is relatively low [8]. Another important attribute is the high estimated average annual productivities for Agave species of 10–34 Mg ha^{-1} $year^{-1}$ in comparison to switchgrass (15 Mg ha^{-1} $year^{-1}$) and poplar wood (11 Mg ha^{-1} $year^{-1}$) [9].

In plants, calcium oxalate deposition is common. Members of more than 215 plant families accumulate crystals within their tissues [10]. Oxalate-producing plants, which include many crop plants, accumulate oxalate in a large mass fraction range (3–80% of their dry weight) [11–14], where as much as 90% of the total calcium of a plant can be found as an oxalate salt [10]. It has been reported that CAM species such as Agave bagasse have higher concentration of calcium oxalate (CaC_2O_4 – CaOX) than most of the current biofuel feedstocks [15] such as grasses (switchgrass), agricultural (sugarcane bagasse) or forestry residues (pine wood) [14,16,17]. Furthermore, these feedstocks does contain realty low to non-measurable elemental calcium content [18–21]. Meanwhile, it has been reported from different Agave species (*americana*, *atrovirens*, *deserti*, *fourcroydes*, *lechugilla*, *salmiana*, *tequilana*, and *utahensis*) ranging from 1.4 to 6.1% of calcium concentration [14,22,23].

Calcium oxalate functions in plants include calcium regulation, plant protection, detoxification (e.g. heavy metals or oxalic acid), ionic equilibrium and tissue support/plant stiffness, even light gathering and its reflection [24]. Another interesting property of calcium oxalate is its exothermic reaction or incompatibility with strong oxidizers such as hydrogen peroxide or ozone, both widely used as solvents or chemicals for biomass pretreatment [24–26]. The presence of high levels of calcium oxalate in agave bagasse could have an effect (positive or negative) on pretreatment performance; hence, this is clearly an important issue to be addressed for future biorefinery applications.

The main objective of this study is to apply raw agave bagasse (*AGB*) as a model (due to its natural high level of CaOX) and CaOX-extracted agave bagasse (*EAB*) to understand the physicochemical changes with both samples in function of biomass pretreatment. An oxidative process, alkaline hydrogen peroxide (*AHP*) and ionic liquid (IL) pretreatments were employed. Lignin removal, crystallinity index using X-ray diffraction (XRD) and chemical fingerprint tracked by Fourier transform infrared spectroscopy (FTIR) were used as response variables, besides, CaOX crystals distribution with scanning electron microscopy with energy dispersive X-ray spectroscopy (SEM-EDS) were carried out. Finally, we conclude with the comparison of sugar yield kinetics of untreated and pretreated biomass.

2. Experimental section

2.1. Experimental design

A 2^4 factorial design with 3 replicates plus controls was used to determine the effect of calcium oxalate on saccharification yields. Four different pretreatment conditions were used namely: *AHP* using two hydrogen peroxide concentrations (*AHP*-A = 125 g kg^{-1} of biomass and *AHP*-B = 500 g kg^{-1} of biomass) and *IL* using two temperatures (*IL*-120 °C and *IL*-160 °C). Two different biomass materials with different calcium oxalate content in agave bagasse samples were applied. On the one hand, named *AGB* (raw agave bagasse without any manipulation that have natural high calcium oxalate concentration) and *EAB* (agave bagasse that was subjected to an extraction process that removed the calcium oxalate). Untreated *AGB* and *EAB* were used as controls. The response variables tested were lignin removal, crystallinity and sugar production.

2.2. Materials and preparation

Agave bagasse was donated by Destilería Rubio, a Tequila plant from Western Mexico in the state of Jalisco. This facility has a year-round process with a real possibility for continues use (6–15 Mg day^{-1}). The central fruit (stem or "piña") was received from defoliated agave plants aged 7–8 years (20°52 46.374 N; 103°49 8.138 O, altitude: 1180 m above sea level, annual rainfall mean 1073 mm; semi-arid climate), located near Tequila, Jalisco. The stems were cooked for 18 h in an autoclave, then milled and compressed to separate the syrup from wet bagasse. Samples of the wet bagasse were collected, washed thoroughly with distilled water and dried in a convection oven at 40 °C. The biomass was milled in a Thomas-Wiley Mini Mill fitted with a 400 μm screen (Model 3383-L10 Arthur H. Thomas Co., Philadelphia, PA, USA). The ground biomass was stored at 4 °C in a sealed plastic bag prior to their use. Cellulases from *Trichoderma reesei* (Celluclast 1.5L with 97 FPU cm^{-3}), β-glucosidase from *Aspergillus niger* (Novozyme 188 with 320 CBU cm^{-3}), 1-Butyl-3-methylimidazolium chloride [C_4C_1Im][Cl], hydrogen peroxide, hydrochloric acid, sulfuric acid, 3,5-dinitrosalicylic acid (DNS), and sodium hydroxide were purchased from Sigma–Aldrich (Mexico). Catalase was purchased from Merck (Mexico).

2.3. Analytical methods and procedures

2.3.1. Calcium oxalate extraction

In order to obtain the extracted agave bagasse (*EAB*) a total calcium oxalate extraction was performed using 1 g of *AGB* into a 250 cm^3 Erlenmeyer flasks and 50 cm^3 of 2 mol dm^{-3} HCl. The flasks were placed in a shaking water bath at 80 °C for 30 min. The extracts where further diluted with 50 cm^3 of deionized water and then transferred into 15 cm^3 centrifuge tubes and centrifuged at 10600× *g* for 10 min [27]. The supernatants were filtered through Whatman #1 filter paper, washed with deionized water and the recovered biomass was vacuum oven dried at 45 °C for 48 h before compositional analysis.

2.3.2. Pretreatment processes

2.3.2.1. IL pretreatment. The ionic liquid [C_4C_1Im][Cl] was purchased from Sigma–Aldrich (≥95% pure), and used without further purification or drying. Pretreatment initiate by mixing 0.3 g of milled biomass with 9.7 g of [C_4C_1Im][Cl] in a 25 cm^3 autoclavable vial using *AGB* and *EAB*. The vials and their contents were heated in an oven (Binder KBF Laboratory oven) at 120 °C and 160 °C for 3 h [28]. All experiments were conducted in triplicates. After 3 h of incubation, 40 cm^3 of deionized water was slowly added into the biomass [C_4C_1Im][Cl] slurry to recover the pretreated biomass. A precipitate immediately formed, and the samples were centrifuged at 10600× *g* for 20–25 min. The supernatant containing *IL* was removed, and the precipitate was washed with water to remove any *IL* excess. The washing process was continued until the concentration of *IL* in the supernatant as measured by Fourier transform infrared (FTIR) spectroscopy was less than 0.2%. The recovered product was vacuum dried at 45 °C for 48 h before compositional analysis.

2.3.2.2. AHP pretreatment. A solution of hydrogen peroxide (H_2O_2) diluted from a commercial 30% stock (Sigma–Aldrich ACS Reagent Grade) was adjusted to pH 11.5 ± 0.2 with 5 mol dm^{-3} NaOH and

mixed with the biomass (*AGB* and *EAB*). Two different concentrations of H_2O_2 were used (*AHP*-A and *AHP*-B) using 1 g of dry biomass plus 10 cm^3 pretreatment solution and their respective NaOH loadings. These conditions were previously determined by Banerjee et al. [25] due to high lignin removal and saccharification yield. All experiments were done in 125 cm^3 flasks at 23 °C (9.43 rad s^{-1} during 48 h). With AHP-A, the pH tended to drift downward, thus the pH was maintained at 11.5 by addition of 5 mol dm^{-3} NaOH every 6 h. After pretreatment, the biomass solutions were neutralized to approximately pH 7 with concentrated HCl, treated with catalase to destroy residual H_2O_2, heated at 90 °C for 15 min to inactivate the catalase, and the recovered product was vacuum dried at 45 °C for 48 h before compositional analysis.

2.3.3. Analysis

2.3.3.1. Chemical characterization. Untreated and pretreated biomass (*AGB* and *EAB*) samples were dried overnight at 80 °C to determine moisture content and heated to 550 °C in a muffle furnace for 24 ± 6 h to determine ash content according to the NREL LAPs: *Preparation of Samples for Compositional Analysis* (NREL/TP-510-42620) and *Determination of Ash in Biomass* (NREL/TP-510-42622). Sugar composition of untreated and pretreated biomass (*AGB* and *EAB*) samples was determined based on a modified NREL LAPs (*Determination of Structural Carbohydrates and Lignin in Biomass*, NREL/TP-510-42618) using a two-step acid hydrolysis. Glucose and xylose were simultaneously measured with an YSI 2700 biochemistry analyzer [29–31]. The content of acid insoluble lignin was measured as the solid residue remaining after two-step hydrolysis. The liquid filtrates were used to determine the content of acid soluble lignin. The acid soluble lignin content was determined with the absorbance at 280 nm and calculated using an averaged extinction coefficient of 1775 $dm^3\ g^{-1}\ cm^{-1}$ [32].

2.3.3.2. Crystallinity measurement. X-ray powder diffraction patterns of untreated and pretreated biomass were collected with an Empyrean diffractometer equipped with a PIXCel detector and operated at 40 kV and 40 mA using Cu-*Kα* radiation. Samples from three replicates were mixed for XRD analysis. Samples were pelletized with a PIKE Crush IR – digital hydraulic press and taped on microscope slides. A reflection-transmission spinner was used as a sample holder and the spinning rate was 0.42 rad s^{-1}. Patterns were collected in the 2θ range of 10–50°, the step size was 0.0167°, and the exposure time was 35 min. Crystallinity index (*CrI*) of untreated and pretreated biomass was determined from XRD data and calculated by curve fitting of the diffraction patterns using the software package HighScore Plus. In order to make an appropriate comparison between *CrI* of untreated and pretreated biomass, the next equation was employed to calculate the percentage of crystallinity relative reduction (*CRR*), as follows:

$$CRR\ (\%) = \frac{Untreated\ biomass\ CrI - Pretreated\ biomass\ CrI}{Untreated\ biomass\ CrI} * 100 \quad (1)$$

where, positive numbers indicate reduction.

2.3.3.3. Attenuated total reflectance (ATR)–FTIR spectroscopy. ATR–FTIR was conducted using a Bruker Optics Vertex system with built-in diamond-germanium ATR single reflection crystal. Untreated and pretreated biomass were pressed uniformly against the diamond surface using a spring-loaded anvil. Sample spectra were obtained in triplicates using an average of 128 scans over the range between 500 cm^{-1} and 2000 cm^{-1} with a spectral resolution of 2 cm^{-1}. Air, water and *IL* solution were used as background for untreated and pretreated biomass samples, respectively. Baseline correction was conducted using the rubberband method following the spectrum minima.

2.3.3.4. Analysis of morphology and elemental analysis. The morphology of untreated biomass was analyzed using a field emission scanning electron microscope (FE-SEM) by a JEOL JSM-7600F equipment. Prior to acquiring images, samples were mounted with doubled sided carbon taped on precut brass sample stubs and coated with approximately 20 nm of gold using a sputtering system in order to avoid static change and kept in a desiccator until analysis. The representative images were acquired with a 7.5 kV and 10 kV accelerating voltage for *AGB* and *EAB*, respectively. Determination of element content was performed with energy dispersive X-ray spectroscopy (EDS), which was carried out in along with SEM imaging.

2.3.3.5. Enzymatic saccharification. Commercially available Celluclast 1.5L and Novozyme 188 enzyme mixtures were used during the saccharification of untreated and pretreated biomass (*AGB* and *EAB*) at 55 °C and 15.71 rad s^{-1} in 0.05 mol dm^{-3} citrate buffer (pH 4.8). Enzyme loading was normalized to the glucan content (5 g glucan dm^{-3}) in the biomass samples to understand the impact of *IL* and *AHP* pretreatment. Enzyme concentration of Celluclast 1.5L and Novozyme 188 were set at 30 FPU g^{-1} of glucan and 60 CBU g^{-1} of glucan, respectively. All assays were performed in triplicate. Error bars show the standard deviation of triplicate measurements.

2.3.3.6. Reducing sugars assay. Saccharification reaction was monitored by taking 50 mm^3 of the saccharification supernatant at specific time intervals (0, 0.5, 1, 3, 6, 24, 48 and 72 h). Collected samples were centrifuged at 10,600× *g* for 5 min, and reducing sugars released during the saccharification were measured by DNS assay. Solutions of D-glucose in water were used as standards [33]. All assays were performed in triplicate. Error bars show the standard deviation of triplicate measurements.

3. Results and discussion

3.1. Composition variability in untreated and pretreated biomass

Changes in chemical composition of *AGB* and *EAB* under different pretreatment conditions using *IL* and *AHP* pretreatment are shown in Table 1. Chemical composition of untreated *AGB* was consistent with other reported values (19.6% of lignin, 21.3% of xylan and 40.5% of glucan) [22,34]. While untreated *EAB* presented similar values for lignin, lower hemicelluloses and enrichment in glucan (19.3% of lignin, 14.8% of xylan and 46.6% of glucan).

EAB resulted in a relative variation of their components, only the ash segment present a significant difference with a ~50% change when compared to *AGB*, probably due to CaOX removal. Both *IL* and *AHP* pretreated biomass when compared to the untreated *AGB* and *EAB* achieved a higher glucan and lower xylan content with *AHP*-A presenting the minors changes. Moreover, *IL* pretreatment was more effective than *AHP* in terms of glucan enrichment obtaining its highest yield at 160 °C decreasing its output with *EAB*. The *EAB* treated at *IL*-160 °C finished with 56.5% of glucan, whereas *AHP* obtained the highest level with *AHP*-B (53.5%). However, the AHP-A process condition only obtained 46.9% of glucan meaning that a higher concentration of hydrogen peroxide contribute to the effectiveness of *AHP* pretreatment. Xylan removal in the pretreated biomass did not represent any interaction between pretreatments obtaining the highest yield with *IL*-160 °C. Therefore *EAB* is determined to be most effective than *AGB* in increasing sugar content and decreasing total lignin content. During *AHP* pretreatment, a significant bubbling occurred only on *EAB* during the first minutes

of both treatments (*AHP*-A and *AHP*-B), which suggested that free microcrystals of CaOX react with H_2O_2, thus liberating CO_2 and water. However, this had the side effect of a lower hydrogen peroxide available for biomass pretreatment. This confirms the incompatibility of CaOX with strong oxidizers that were still present after the washing step during the CaOX extraction process, as shown in the biomass morphology section [24]. On the other hand using IL pretreatment in *EAB* did not have any interaction with the CaOX as *ILs* are not oxidative agents.

3.2. Effect of material and pretreatment on biomass delignification

Lignin interferes with biomass saccharification in nature and in biofuel production by occluding and protecting cellulose fibers from depolymerization. Lignin also binds and inactivates cellulolytic enzymes and can produce degradation products that inhibit further fermentation [35]. A decrease as function of pretreatment severity was obtained. The highest lignin removal for each pretreatment in both materials occurred with *IL*-160 °C and *AHP*-B. In terms of biomass type, based on 19.6% (untreated *AGB*) and 19.3% (untreated *EAB*) the highest difference of total lignin occurred with *IL*-160 °C with 17.2% and 15.4% for *AGB* and *EAB*, respectively. Hence, *IL* pretreatment was more effective than *AHP* in decreasing lignin content from the biomass and an increase occurred with *EAB* when compared to *AGB* with both pretreatments. Differences in lignin content of untreated vs. pretreated *AGB* is lower when compared to another report where untreated *AGB* was 19.9% of lignin and IL-pretreated AGB with $[C_2C_1Im][OAc]$ at 120 and 160 °C was 16.7 and 12.8% of lignin, respectively [15]. We hypothesize that the differences in the reported delignification efficiency are likely due to the following reasons: (1) a high content of CaOX in the agaves could interfere in the oxidative pretreatment due to the recalcitrance of the biomass. This recalcitrance is largely governed by the relative composition and proportions of the cell wall components like cellulose, lignin, hemicellulose, among others, as well as the interactions between these polymers [36], (2) employing higher temperatures in *IL* from 120 to 160 °C, proportion of H_2O_2 in *AHP* and incubation times, presented more effective pretreatments, indicating that there may be effective lignin glass transition temperature that must be exceeded to efficiently solubilize lignin, (3) a decreased cellulose crystallinity as reported in the following chapter and (4) the interactions of specific ionic liquids with biomass depended on the cation, anion, temperature, and time used in the pretreatment process.

Fig. 1 shows the FTIR spectroscopy used to track changes in chemical composition of the pretreated and untreated biomass samples and relative changes in chemical compositions of the solids from *IL* and *AHP* pretreatments along with the assignment of band positions are shown in Supporting material Tables SI and SII for *AGB* and *EAB*, respectively. For ATR–FTIR data, six unique lignin and carbohydrate specific bands are used to monitor the chemical changes plus two additional ones for calcium oxalate, as well as the amorphous to crystalline cellulose ratio. The band position attributed to CaOX at 1321 and 1622 cm^{-1} was present as expected in *AGB* while *EAB* show minor intensities from the effectiveness of the CaOX extraction process [16,37]. The relative change in the pretreated *AGB* in terms of the calcium oxalate bands was significantly higher with *IL* when compared to *AHP*. In contrast with the untreated samples, both pretreatment processes decrease the CaOX peak intensities. In *AGB*, *IL* pretreatment show higher decrease for the CaOX bands than *AHP* pretreatment. The peak at 900 cm^{-1} (anti-symmetric out-of plane ring stretch of amorphous cellulose) observed in the spectra of *IL* pretreated samples of *AGB*, which reflects the relative increase in cellulose content as a result of partial removal of both lignin and hemicellulose. The band at 1745 cm^{-1} which is associated with carbonyl C=O stretching decreased for *AHP* to a similar extent for *AGB* and *EAB*, indicating more cleavage of lignin removal and side chains [38]. However, the band at 1510 cm^{-1} (aromatic skeletal from lignin) could not be effectively determined in *AGB* due to a peak overlap of the lignin peak by the high intensity calcium oxalate peak. Event that did not occurred with *EAB* due to calcium oxalate extraction. Finally, decreases occurred in the intensities of the bands at 1375 cm^{-1} (C–H deformation in cellulose & hemicellulose) and 1056 cm^{-1} (C–O stretch in cellulose & hemicellulose) with both pretreatments in *AGB* and *EAB*, being higher with *IL* pretreatment probably due to xylan removal [39]. The ratio intensities at the bands 900 and 1098 cm^{-1} are dependent on pretreatment condition that can alter the ratio of amorphous to crystalline cellulose.

3.3. Effect of pretreatment on biomass crystallinity

X-ray diffraction (XRD) patterns of *AGB* and *EAB* are shown in Fig. 2. Crystallinity of cellulosic biomass has been reported to affect enzymatic saccharification and its efficiency [40]. Various pretreatments have been shown to change cellulose crystallinity and cellulose structure in the biomass by disrupting inter- and intra-chain hydrogen bonding of cellulose fibrils [41].

Cellulose crystallinity index (*CrI*) and cellulose polymorph present in the biomass is based on the assumption that there is only a single crystalline phase present along an amorphous phase. The diffraction pattern of *AGB* displays prominent peaks of CaOX at

Table 1
Polymer and ash mass fractions (%) of untreated and pretreated biomass (agave bagasse and extracted agave bagasse).

	Glucan	Xylan	Total lignin[a]	Acid-soluble lignin	Acid-insoluble lignin	Ashes
Agave bagasse (*AGB*)						
Untreated	40.5 ± 0.5	21.3 ± 0.4	19.6 ± 0.9	3.6 ± 0.3	16.0 ± 0.6	6.4 ± 0.2
AHP-A[b]	40.8 ± 0.7	19.9 ± 0.6	18.5 ± 0.4	2.8 ± 0.2	15.7 ± 0.2	8.8 ± 0.2
AHP-B[c]	44.5 ± 0.7	18.9 ± 0.2	17.6 ± 0.1	2.5 ± 0.0	10.3 ± 0.1	4.5 ± 0.3
IL-120 °C	49.9 ± 0.7	19.2 ± 0.0	17.3 ± 0.2	2.5 ± 0.1	14.8 ± 0.1	4.3 ± 0.4
IL-160 °C	52.5 ± 0.4	18.6 ± 0.1	17.2 ± 0.1	2.5 ± 0.0	14.7 ± 0.1	4.0 ± 0.3
Extracted agave bagasse (*EAB*)						
Untreated	46.6 ± 0.5	14.8 ± 0.1	19.3 ± 0.3	4.1 ± 0.1	15.2 ± 1.4	2.8 ± 0.6
AHP-A[b]	46.9 ± 0.6	13.2 ± 0.5	18.2 ± 0.4	3.4 ± 0.2	14.8 ± 0.3	3.1 ± 0.3
AHP-B[c]	58.9 ± 0.3	10.9 ± 0.3	17.4 ± 0.7	2.1 ± 0.2	15.3 ± 0.5	2.7 ± 0.4
IL-120 °C	53.5 ± 0.4	11.6 ± 0.1	15.8 ± 0.2	1.9 ± 0.0	13.9 ± 0.2	2.2 ± 0.8
IL-160 °C	56.5 ± 0.4	10.6 ± 0.0	15.4 ± 0.2	1.8 ± 0.1	13.6 ± 0.1	1.9 ± 0.9

[a] Total lignin = acid soluble lignin + acid insoluble lignin.
[b] Alkaline hydrogen peroxide using 125 g kg^{-1} of biomass.
[c] Alkaline hydrogen peroxide using 500 g kg^{-1} of biomass.

2θ = 15°, 24.5° and 30.5°, which correspond to the (10−1), (020) and (20−2) lattice planes in monoclinic CaOX.

Calcium oxalate extraction process efficiency can be confirmed using the diffraction pattern of *EAB* where a notable reduction in each of the CaOX peaks is evident. Crystallinity index of the cellulose I lattice was estimated using software to separate amorphous and crystalline contributions to the diffraction spectrum using a curve-fitting process. The *CrI* of untreated *AGB* was 39% with a reduction in the pretreated samples 35% of *AHP*-A, 34% of *AHP*-B, 28% of *IL*-120 °C and 17% of *IL*-160 °C.

In contrast, the *EAB* achieved a lower *CrI* than *AGB*. The *CrI* of untreated *EAB* was 28% and the pretreated samples are: 30% (*AHP*-A), 29% (*AHP*-B), 14% (*IL*-120 °C) and 11% (*IL*-160 °C). Only on the *IL* pretreated samples in *EAB* at 120 °C and 160 °C, the main peak at around 22.0° shifted to a lower angle (21.2°) and became broader. Perez-Pimienta et al. [7] reported a shift in the main peak for 3% of $[C_2C_1Im][OAc]$ at 120 °C for 3 h in *AGB*. The broad peak dropped its intensity and became a weak shoulder peak at around 16.0°. However, the *CrI* in the *IL* pretreated sample at 160 °C in both *AGB* (17%) and *EAB* (11%) did not achieved a decrease in crystallinity as low as 9% at the same temperature and time using $[C_2C_1Im][OAc]$ as shown in the same report.

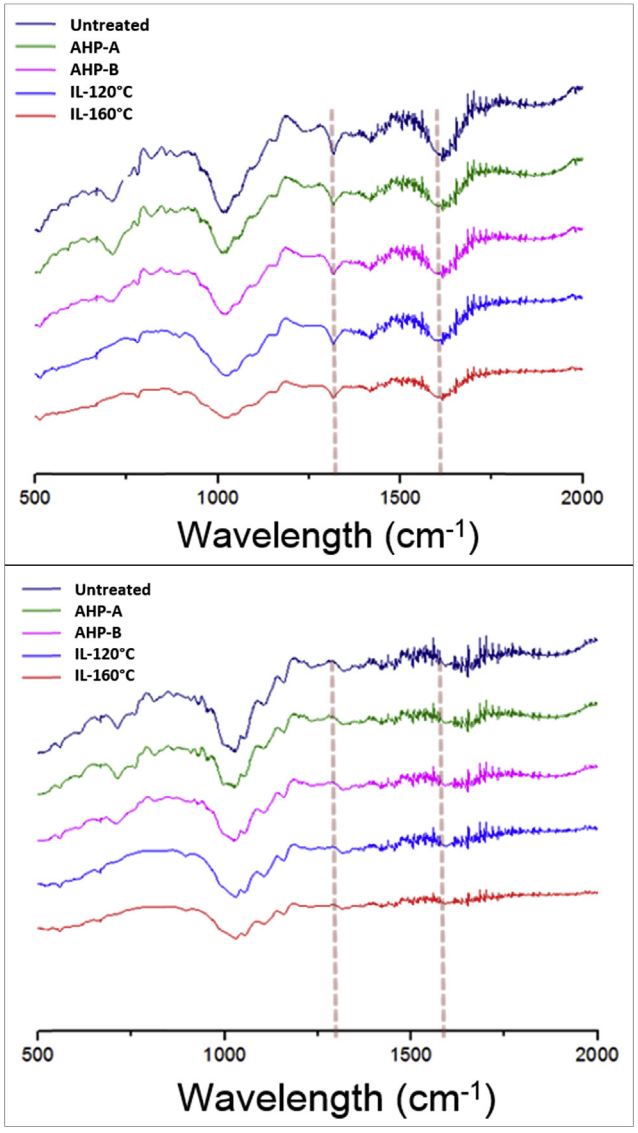

Fig. 1. Chemical changes tracked of untreated and pretreated agave bagasse (top) and extracted agave bagasse (bottom), as determined by FTIR. Calcium oxalate bands are outlined (1321 and 1622 cm^{-1}).

A decrease in crystallinity due to these changes is consistent with severe distortion of cellulose I lattice [42]. Fig. 3 presents the percentage of crystallinity relative reduction (*CRR*) of *IL* and *AHP* pretreated samples of *AGB* and *EAB*. The *CRR* of the *AGB* presented positive numbers for both *IL* and *AHP*, whereas, in the *EAB* only the *IL* pretreatment achieved positive *CRR* but not in *AHP* pretreatment where there was a reduction up to 7%. During the *AHP* pretreatment using *AHP*-A and *AHP*-B achieved similar *CRR* values for *AGB* (10 and 13%). Similarly, but in negative values for *EAB* was −7 and −4% (*AHP*-A and *AHP*-B, respectively) indicating that a lower crystallinity could be obtained at a higher concentration of H_2O_2. Moreover, the *IL* pretreatment obtained the highest *CRR* at 160 °C for both *AGB* (56%) and *EAB* (61%) whereas at 120 °C were 28% and 50% for *AGB* and *EAB*, respectively. Furthermore, the *CRR* for *IL* pretreatment at 160 °C in *AGB* and *EAB* achieved similar values with only a minor difference (~5%) in comparison to *IL*-120 °C (~22%). All these results suggest that CaOX provides a specific recalcitrance for agave bagasse and its removal could lead to a lower *CrI* in *IL* pretreatment.

3.4. Effect of pretreatment on biomass morphology

SEM images were taken using a magnification of 5,000× and 1,000× of untreated *AGB* and *EAB*, respectively, to deduce the CaOX crystals distribution (Supporting material, Figs. SI-A and SI-B). Calcium oxalate crystals of ~1 μm in considerable quantities were found in untreated *AGB* mainly in the form of styloid crystals dispersed along the surface which are consistent with previous reports [43]. Environmental conditions influence the quantity of calcium oxalate produced and the number of crystals formed which in the genre agave are stored in deposits located on the cuticular surface, which may be present in various forms, either as druses (composite shapes), styloid (elongated simple) and raphides (elongated in aggregate), which becomes a defense system against insects and animals. These compounds are the main agents of dermatitis in handling plant workers in the tequila industry [44]. In contrast, the SEM images of untreated *EAB* present notable differences when compared to *AGB*; in this case it is evident the presence of free calcium oxalate crystals separated from the plant cell wall and reaching large size (~20 μm). As a result of the extraction process, the growth of the {001} pinacoid planes is stabilized resulting in large {001} faces and truncated {101} faces as identified in isolated CaOX crystals by Pennisi et al. [45]. We show this structure in Supporting material Fig. SI-C. We can hypothesize that free CaOX crystals in *EAB* could have reacted with the H_2O_2 during the *AHP* pretreatment, resulting in a reduced sugar yield in comparison to *AGB*, in which CaOX crystals remained tightly attached to the plant cell wall. Additionally, elemental analysis (weight percentages) using EDS showed that *AGB* contains a high percentage of calcium (4.7%) in addition to 51.5% of C and 43.8% of O when compared to current biofuel feedstocks (with really low to non-measurable Ca amounts) [18–20] but lower than *Opuntia* with values above 6% [14,23]. Furthermore, calcium content of *AGB* are within the range of others agave species ranging 1.7–6.1% [14,23]. On the other hand, EDS analysis (weight percentages) of *EAB* showed that Ca was removed from the plant cell wall after extraction, only 70.7% of C and 27.7% of O remains with trace amounts of others elements.

3.5. Effect of pretreatment on sugar production

Saccharification experiments were carried out using *IL* and *AHP*

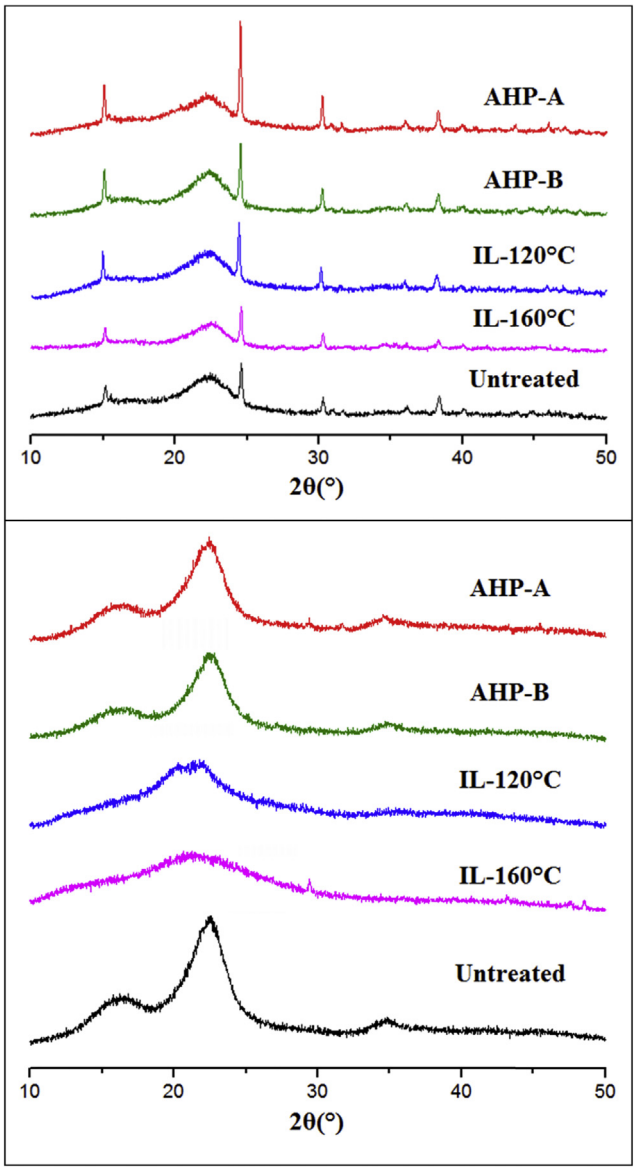

Fig. 2. X-ray diffractograms of untreated and pretreated agave bagasse (top) and extracted agave bagasse (bottom).

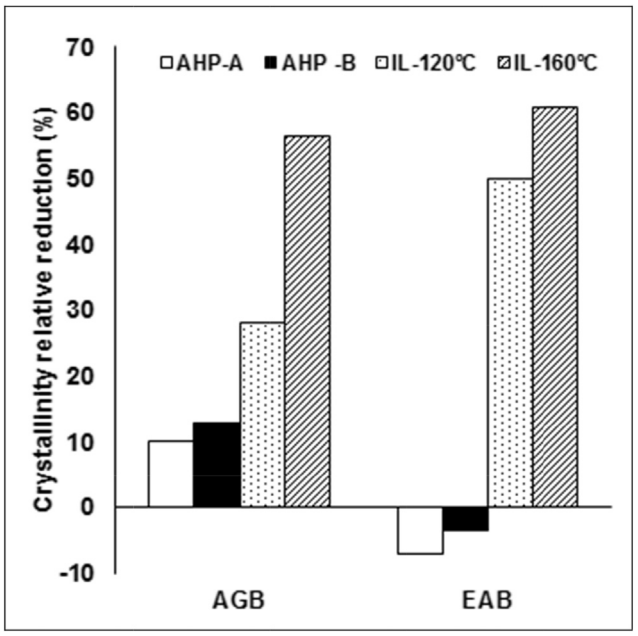

Fig. 3. Effect of ionic liquid and alkaline hydrogen peroxide pretreatment on agave bagasse and extracted agave bagasse in the percentage of crystallinity relative reduction.

pretreated biomass with commercial enzyme cocktails in order to compare their digestibility using a normalized glucan content (5 g dm^{-3}). Sugar production profiles for untreated and pretreated biomass are available in Supporting material Fig. SII. When compared to the untreated samples both pretreatments (*IL* and *AHP*) were effective to obtain higher sugar yield in *AGB* and *EAB* due to lower lignin content and crystallinity. Sugar production kinetics from *EAB* reached their highest values with IL pretreatment when compared to *AHP*, inverse to those obtained with *AGB* under the same conditions.

Sugar production at 72 h from untreated and pretreated of both samples (*AGB* and *EAB*) is summarized in Fig. 4. The highest production of reducing sugars during enzymatic saccharification for each pretreatment was obtained for *EAB* with *IL-120* °C (7.8 g dm^{-3}) followed by *AGB* with *AHP-B* (6.9 g dm^{-3}). It should be noted that it was expected the opposite results in both samples, obtaining the highest yield with *AHP* and *IL* pretreatment for *AGB* and *EAB*, respectively. Due to the oxidative characteristics of *AHP* pretreatment, the hydrogen peroxide was expected to react with the CaOX contained on the *AGB* cell wall, however, this was not the case. Instead, the H_2O_2 interacted with the free CaOX microcrystals on *EAB*, hence, we can infer that were detached from the plant cell wall (based on SEM-EDS analysis), and finally consumed, turning *AHP* pretreatment into a less effective process. Finally, a noticeable reduction on the final sugar yield of *AHP*-pretreated *EAB* occurred (by ca 39%) when compared to *AGB*. Hence, when *AGB* is applied to biorefineries schemes using *AHP* (at the applied conditions) would not cause any effect in the AGB-CaOX, obtaining high lignin removal and sugar yields. However, further studies are necessaries to uncover CaOX mechanism using higher H_2O_2 concentration (or similar oxidants such as ozone) with elevated CaOX levels materials such as *AGB* or *Opuntia*.

Calcium oxalate extraction in terms of pretreatment has an effect showing improving sugar production and faster enzymatic hydrolysis with *AHP* in *AGB* and *IL* in *EAB*. Sugar yield increase in the saccharification can be attributed to: (1) lignin removal and xylan depolymerization, (2) reduced cellulose crystallinity, most notorious on the *EAB* samples resulted in amorphous cellulose that provides an enhanced surface area leading to a better enzyme accessibility, (3) *EAB* resulted in an effective recovered product in terms of lignin removal and crystallinity during *IL* pretreatment than with *AGB* (that had higher natural levels of calcium oxalate), and (4) calcium oxalate extraction results in more free accessible area to enzymes that could react on the cellulose.

4. Conclusions

Effects of CaOX on IL and AHP pretreatment of *AGB* and *EAB* have been systematically investigated in terms of physicochemical changes and enzymatic saccharification. Compositional analysis indicated delignification, partial xylan removal and glucan enrichment for both *IL* and *AHP* pretreatments. A lower biomass crystallinity was achieved after pretreatment in both *AGB* and *EAB*. Removal of CaOX extraction in *AGB* had a positive effect in terms of sugar production for the IL pretreatment using $[C_4C_1Im][Cl]$, while

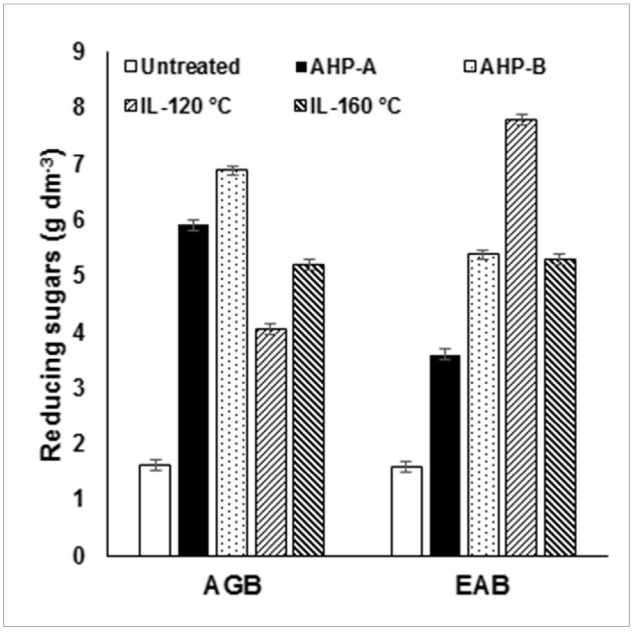

Fig. 4. Sugar production at 72 h with untreated and pretreated biomass (agave bagasse (*AGB*) and extracted agave bagasse (*EAB*) with ionic liquid and alkaline hydrogen peroxide.

AHP reacted negatively to free CaOX crystals detached from the *AGB* cell wall. Hence, this study indicates that an oxidative pretreatment such as AHP at the applied conditions would not cause any effect in the AGB-CaOX thus obtaining high lignin removal and sugar yields. However, further studies are necessaries to uncover CaOx mechanism using higher levels of H_2O_2 (or similar oxidants such as ozone) applied in elevated CaOX levels materials such as *AGB* or *Opuntia*.

Acknowledgements

The authors acknowledge support by the Consejo Nacional de Ciencia y Tecnología Mexico (CONACyT) for Grant CB/14-236895 and Cinvestav-IPN, Mexico for partial funding this study. This work was part of the DOE Joint BioEnergy Institute (http://www.jbei.org) supported by the U. S. Department of Energy, Office of Science, Office of Biological and Environmental Research, through contract DE-AC02-05CH11231 between Lawrence Berkeley National Laboratory and the U. S. Department of Energy.

Appendix A. Supplementary data

Supplementary data related to this article can be found at http://dx.doi.org/10.1016/j.biombioe.2016.05.001.

References

[1] V.R. Pallapolu, Y.Y. Lee, R.J. Garlock, V. Balan, B.E. Dale, Y. Kim, et al., Effects of enzyme loading and β-glucosidase supplementation on enzymatic hydrolysis of switchgrass processed by leading pretreatment technologies, Bioresour. Technol. 102 (2011) 11115–11120.
[2] J.S. Kim, Y.Y. Lee, T.H. Kim, A review on alkaline pretreatment technology for bioconversion of lignocellulosic biomass, Bioresour. Technol. 199 (2015) 42–48.
[3] P. Kumar, D.M. Barrett, M.J. Delwiche, P. Stroeve, Methods for pretreatment of lignocellulosic biomass for efficient hydrolysis and biofuel production, Ind. Eng. Chem. Res. 48 (2009) 3713–3729.
[4] A.A. Elgharbawy, Z. Alam, M. Moniruzzaman, M. Goto, Ionic liquid pretreatment as emerging approaches for enhanced enzymatic hydrolysis of lignocellulosic biomass, Biochem. Eng. J. 109 (2016) 252–267.
[5] S.P. Long, Light to liquid fuel: theoretical and realized energy conversion efficiency of plants using crassulacean acid metabolism (CAM) in arid conditions, J. Exp. Bot. 65 (2014) 3471–3478.
[6] A.M. Borland, H. Griffiths, J. Hartwell, J.A.C. Smith, Exploiting the potential of plants with crassulacean acid metabolism for bioenergy production on marginal lands, J. Exp. Bot. 60 (2009) 2879–2896.
[7] J.A. Perez-Pimienta, M.G. Lopez-Ortega, P. Varanasi, V. Stavila, G. Cheng, S. Singh, et al., Comparison of the impact of ionic liquid pretreatment on recalcitrance of agave bagasse and switchgrass, Bioresour. Technol. 127 (2013) 18–24.
[8] F. Sun, M.L. Roderick, G.D. Farquhar, W.H. Lim, Y. Zhang, N. Bennett, et al., Partitioning the variance between space and time, Geophys. Res. Lett. 37 (2010) n/a–n/a.
[9] H. Li, M.B. Foston, R. Kumar, R. Samuel, X. Gao, F. Hu, et al., Chemical composition and characterization of cellulose for Agave as a fast-growing, drought-tolerant biofuels feedstock, RSC Adv. 2 (2012) 4951.
[10] P.A. Nakata, Advances in our understanding of calcium oxalate crystal formation and function in plants, Plant Sci. 164 (2003) 901–909.
[11] B. Libert, V.R. Franceschi, Oxalate in crop plants, J. Agric. Food Chem. 35 (1987) 926–938.
[12] R.P. Holmes, M. Kennedy, Estimation of the oxalate content of foods and daily oxalate intake, Kidney Int. 57 (2000) 1662–1667.
[13] K. Judprasong, S. Charoenkiatkul, P. Sungpuag, K. Vasanachitt, Y. Nakjamanong, Total and soluble oxalate contents in Thai vegetables, cereal grains and legume seeds and their changes after cooking, J. Food Compos. Anal. 19 (2006) 340–347.
[14] P.S. Nobel, W.L. Berry, Element responses of agaves, Am. J. Bot. 72 (1985) 686–694.
[15] J.A. Perez-Pimienta, M.G. Lopez-Ortega, J.A. Chavez-Carvayar, P. Varanasi, V. Stavila, G. Cheng, et al., Characterization of agave bagasse as a function of ionic liquid pretreatment, Biomass Bioenergy 75 (2015) 180–188.
[16] P.V. Monje, E.J. Baran, Characterization of calcium oxalate biominerals in Pereskia species (Cactaceae), Z. Fur Naturforschung – Sect. C J. Biosci. 64 (2010) 763–766.
[17] P.S. Nobel, Nutrient levels in cacti-relation to nocturnal acid accumulation and growth, Am. J. Bot. 70 (1983) 1244–1253.
[18] S. Darmawan, N.J. Wistara, G. Pari, A. Maddu, W. Syafii, Characterization of Lignocellulosic Biomass as Raw Material for the Production of Porous Carbon-based, vol. 11, 2016, pp. 3561–3574.
[19] K. David, A.J. Ragauskas, Switchgrass as an energy crop for biofuel production: a review of its ligno-cellulosic chemical properties, Energy Environ. Sci. 3 (2010) 1182–1190.
[20] D. Medic, M. Darr, A. Shah, S. Rahn, The effects of particle size, different corn stover components, and gas residence time on torrefaction of corn stover, Energies 5 (2012) 1199–1214.
[21] C.T. Yu, W.H. Chen, L.C. Men, W.S. Hwang, Microscopic structure features changes of rice straw treated by boiled acid solution, Ind. Crops Prod. 29 (2009) 308–315.
[22] A.I. Ávila-Lara, J.N. Camberos-Flores, J.A. Mendoza-Pérez, S.R. Messina-Fernández, C.E. Saldaña-Duran, E.I. Jimenez-Ruiz, et al., Optimization of alkaline and dilute acid pretreatment of agave bagasse by response surface methodology, Front. Bioeng. Biotechnol. 3 (2015).
[23] A. Bernardino-Nicanor, G. Teniente-Martínez, J. Juarez-Goiz, S. Filardo-Kerstupp, J. Montañez-Soto, L. González-Cruz, Changes in the concentration and characteristics of calcium oxalate crystals during development stages of Agave atrovirens, Adv. Biores. 3 (2012) 22–28.
[24] V.R. Franceschi, P.A. Nakata, Calcium oxalate in plants: formation and function, Annu. Rev. Plant Biol. 56 (2005) 41–71.
[25] G. Banerjee, S. Car, J.S. Scott-Craig, D.B. Hodge, J.D. Walton, Alkaline peroxide pretreatment of corn stover: effects of biomass, peroxide, and enzyme loading and composition on yields of glucose and xylose, Biotechnol. Biofuels 4 (2011) 16.
[26] R. Travaini, M.D.M. Otero, M. Coca, R. Da-Silva, S. Bolado, Sugarcane bagasse ozonolysis pretreatment: effect on enzymatic digestibility and inhibitory compound formation, Bioresour. Technol. 133 (2013) 332–339.
[27] I.A. Al-Wahsh, Y. Wu, M. Liebman, A comparison of two extraction methods for food oxalate assessment, J. Food Res. 1 (2012) 233–239.
[28] C. Li, G. Cheng, V. Balan, M.S. Kent, M. Ong, S.P.S. Chundawat, et al., Influence of physico-chemical changes on enzymatic digestibility of ionic liquid and AFEX pretreated corn stover, Bioresour. Technol. 102 (2011) 6928–6936.
[29] A. Sluiter, B. Hames, R. Ruiz, C. Scarlata, Determination of Structural Carbohydrates and Lignin in Biomass, Laboratory Analytical Procedure, National Renewable Energy Laboratory, Golden, CO, 2008. NREL/TP-510-42618. 2011, http://www.nrel.gov/biomass/pdfs/42618.pdf.
[30] A. Sluiter, B. Hames, R.O. Ruiz, C. Scarlata, J. Sluiter, D. Templeton, et al., Determination of Ash in Biomass, in: Biomass Analysis Technology Team Laboratory Analytical Procedure, 2004, pp. 1–6.
[31] B. Hames, R. Ruiz, C. Scarlata, a Sluiter, J. Sluiter, D. Templeton, Preparation of samples for compositional analysis laboratory analytical procedure (LAP) issue date : 8/06/2008 preparation of samples for compositional analysis laboratory analytical procedure (LAP), Renew. Energy (2008) 1–12.
[32] R.S. Fukushima, R.D. Hatfield, Comparison of the acetyl bromide spectrophotometric method with other analytical lignin methods for determining lignin concentration in forage samples, J. Agric. Food Chem. 52 (2004) 3713–3720.
[33] G.L. Miller, Use of dinitrosalicylic acid reagent for determination of reducing sugar, Anal. Chem. 31 (1959) 426–428.

[34] S.C. Davis, F.G. Dohleman, S.P. Long, The global potential for Agave as a biofuel feedstock, GCB Bioenergy 3 (2011) 68–78.
[35] N. Sorek, T.H. Yeats, H. Szemenyei, H. Youngs, C.R. Somerville, The implications of lignocellulosic biomass chemical composition for the production of advanced biofuels, BioScience 64 (2014) 192–201.
[36] S. Pattathil, M.G. Hahn, B.E. Dale, S.P.S. Chundawat, Insights into plant cell wall structure, architecture, and integrity using glycome profiling of native and AFEX™-pretreated biomass, J. Exp. Bot. 66 (2015) 4279–4294.
[37] A. Nevin, J.L. Melia, I. Osticioli, G. Gautier, M.P. Colombini, The identification of copper oxalates in a 16th century Cypriot exterior wall painting using micro FTIR, micro Raman spectroscopy and Gas Chromatography-Mass Spectrometry, J. Cult. Herit. 9 (2008) 154–161.
[38] R. Kumar, G. Mago, V. Balan, C.E. Wyman, Physical and chemical characterizations of corn stover and poplar solids resulting from leading pretreatment technologies, Bioresour. Technol. 100 (2009) 3948–3962.
[39] C. Li, B. Knierim, C. Manisseri, R. Arora, H.V. Scheller, M. Auer, et al., Comparison of dilute acid and ionic liquid pretreatment of switchgrass: biomass recalcitrance, delignification and enzymatic saccharification, Bioresour. Technol. 101 (2010) 4900–4906.
[40] G. Cheng, P. Varanasi, C. Li, H. Liu, Y.B. Melnichenko, B.A. Simmons, et al., Transition of cellulose crystalline structure and surface morphology of biomass as a function of ionic liquid pretreatment and its relation to enzymatic hydrolysis, Biomacromolecules 12 (2011) 933–941.
[41] N. Mosier, C. Wyman, B. Dale, R. Elander, Y.Y. Lee, M. Holtzapple, et al., Features of promising technologies for pretreatment of lignocellulosic biomass, Bioresour. Technol. 96 (2005) 673–686.
[42] G. Cheng, P. Varanasi, R. Arora, V. Stavila, B.A. Simmons, M.S. Kent, et al., Impact of ionic liquid pretreatment conditions on cellulose crystalline structure using 1-ethyl-3-methylimidazolium acetate, J. Phys. Chem. B 116 (2012) 10049–10054.
[43] C.J. Prychid, P.J. Rudall, Calcium oxalate crystals in monocotyledons, A Rev. Ann. Bot. 84 (1999) 725–739.
[44] M.L. Salinas, T. Ogura, L. Soffchi, Irritant contact dermatitis caused by needle-like calcium oxalate crystals, raphides, in Agave tequilana among workers in tequila distilleries and agave plantations, Contact Dermat. 44 (2001) 94–96.
[45] S.V. Pennisi, D.B. McConnell, L.B. Gower, M.E. Kane, T. Lucansky, Intracellular calcium oxalate crystal structure in *Dracaena sanderiana*, New Phytol. 149 (2001) 209–218.